

# Seismic Response of Multi-Story Structure With Semi-Active Multiple Tuned Mass Friction Dampers

Alka Y. Pisal<sup>1</sup> and R. S. Jangid<sup>2</sup>

<sup>1</sup> Research Scholar , <sup>2</sup> Professor

<sup>1,2</sup>Department of Civil Engineering, Indian Institute of Technology Bombay, Powai, Mumbai - 400 076, India

## ABSTRACT

A passive tuned mass friction damper (P-TMFD) has a pre-determined and fixed slip force at which it controls the response of the structure effectively and at any other values it loses its efficiency. To overcome this disadvantage, semi-active multiple tuned mass friction dampers (SA-MTMFDs) are proposed. The predictive control law is used for the semi-active system, so that it can produce continuous and smooth slip forces and eliminates the high frequency response of the structure which usually occurs in case of passive multiple tuned mass friction dampers (P-MTMFDs). Also, the effectiveness of SA-MTMFDs over P-MTMFDs is investigated. The governing differential equations of motion are solved numerically using the state-space method. The response of a five story shear type structure is investigated for four considered earthquake ground motions. The number of tuned mass friction damper (TMFD) units of SA-MTMFDs and P-MTMFDs are varied and the responses of the five story structure with SA-MTMFDs are compared with the responses of the same structure with the P-MTMFDs. For a fair comparison the displacement and acceleration response time histories of the structure with SA-MTMFDs and P-MTMFDs are compared with respect to their optimum controlling parameters. The result of numerical studies indicated that the SA-MTMFDs are more effective and has better performance level than the P-MTMFDs for same input seismic excitations.

**KEYWORDS:** P-MTMFDs, SA-MTMFDs, predictive control, numerical analysis, seismic excitation, optimum parameters and response reduction.

## I. INTRODUCTION

The tuned mass damper (TMD) is a most popular and extensively used device to control vibrations in civil and mechanical engineering applications ranging from small rotating machinery to tall civil engineering structures. Similar to TMD, friction dampers (FD) were found to be very efficient, not only for rehabilitation and strengthening of existing structures but also for the design of structures to resist excessive vibrations (Colajanni and Papia, 1995; Qu et al., 2001; Mulla and Belev, 2002; Pasquin et al., 2004). In the past, some researchers had proposed the use of FD along with TMD. Ricciardelli and Vickery (1999) considered a SDOF system to which a TMD with linear stiffness and dry friction damping was attached. The system was analyzed for harmonic excitation and design criteria for friction TMD system were proposed. Lee et al. (2005) performed a feasibility study of tunable friction damper. Gewei and Basu (2010) used harmonic and static linearization solutions to analyze dynamic characteristics of SDOF system with friction tuned mass damper. P-TMFD is having advantage that it can behave either as a FD when it is in slip-state and as an added mass when it is in stick state. On the other hand, the main disadvantage of a single P-TMFD is its sensitivity of the effectiveness to the error in the natural frequency of the structure. If the design parameters of the TMD are chosen wrongly, it may accelerate the vibration of the system instead of attenuating it. To overcome this difficulty, many researchers proposed the use of more than one TMD with different dynamic characteristics, (Xu and Igusa, 1992; Joshi and Jangid, 1997). They proved that MTMDs are more effective than single TMD. The another disadvantage of P-TMFDs is that it has a pre-determined and a fixed value of slip force at which it reduces the response of the system to which it is attached, when it is in slip mode. At too small and too high value of slip force, the damper will not slip for the most of the harmonic and earthquake excitation duration and thus the capacity of P-TMFDs to reduce structural response may not be fully utilized. Also during an earthquake P-TMFD vibrate in two different modes (i.e. stick state and slip state), many times which results in high-frequency structural responses which are undesirable.

In order to improve the performance of such passive devices, the concept of semi-active control was emerged. The advantage of semi-active control system is that it is able to adjust its slip force by controlling its clamping force in real time with respect to the response of the structure during an excitation. Dowdell and Cherry (1994) and Kannan et al. (1995) were among the first researchers to study the response of structures with semi-active friction dampers. They adopted on-off and bang-bang control methods for their study. Inaudi (1997) proposed modulated homogeneous friction control algorithm which produces a slip force proportional to the prior local peak of the damper deformation. Akbay and Aktan (1995) proposed a control algorithm that determines the clamping force in next time step by one pre-specified increment of the current force at a fixed time step. Also, the literature review shows that the control performance of semi-active dampers fully depends on the applied control algorithm. There have been many studies on the development of the control law. From the review of the literature of these studies, it is clear that most of the developed algorithm either produces the discontinuous control forces or partially continuous slip forces. In both the cases the damper capacity may not be fully used. Recently, Lin et al. (2010) proposed SAF-TMD and investigated the effectiveness of SAF-TMD in protecting structures subjected to seismic forces using non-sticking law.

It is also observed that the semi-active control algorithms are developed specifically for TMD and for FD, but limited algorithms are developed for MTMFDs. In this study, the performance of SA-MTMFDs attached to a damped five story shear type structure is investigated for seismic ground excitations. The control algorithm developed by Lu (2004), known as predictive control is applied to SA-MTMFDs to get a continuous smooth slip force, so that it remains in its slip state during entire earthquake duration. The specific objectives of the study are summarized as (i) to formulate the equations of motion and obtained the response of Multi-story structure with SA-MTMFDs, under seismic excitations, (ii) to identify a appropriate parameter which controls the desired responses of the multi-story structure with SA-MTMFDs, (iii) to investigate the effect and optimum value of gain multiplier for the response reduction of the controlled multi-story structure and (iv) to investigate the effectiveness of SA-MTMFDs in response reduction under the earthquake excitations.

## II. MODELING OF MDOF SYSTEM WITH SA-MTMFDS

The system configuration considered for the study consists of a primary system of five story shear structure attached with SA-MTMFDs with different dynamic characteristics as shown in Figure 1. The  $i^{th}$  floor of primary structure is characterized by mass  $m_i$ , stiffness  $k_i$  and fundamental frequency  $\omega_s$ . The mass, stiffness and natural frequency of  $j^{th}$  SA-TMFD unit is shown as  $m_{Td j}$ ,  $k_{Td j}$  and  $\omega_{Td j}$ , respectively. The primary structure and each SA-TMFD unit are modeled as single degree of freedom system (SDOF) so that the total degrees of freedom of the system configuration considered for the study is  $r+n$  where,  $r$  denotes the number of TMFD units and  $n$  denotes the number of degrees of primary structure. For the present study, the following assumptions are made:

- [1] The structural configuration of the primary system i.e. mass and stiffness of each floor are same. Also, the damping ratio for each mode of vibration is assumed to be constant.
- [2] Stiffness of each SA-TMFD unit is same.
- [3] The mass of each SA-TMFD unit is varying. By keeping the stiffness of each SA-TMFD constant and varying the mass, we vary the natural frequency of each SA-TMFD unit.
- [4] The natural frequencies of the SA-TMFDs are uniformly distributed around their average natural frequency. It is to be noted that SA-MTMFDs with indistinguishable dynamic characteristics are equivalent to a single SA-TMFD in which the natural frequency of the individual SA-MTMFD unit is same as that of the equivalent single SA-TMFD.
- [5] The SA-TMFD units apply variable friction force on the primary system, which can be controlled by varying the clamping force.

However, the mass and friction force is the sum of all the SA-MTMFDs masses and friction forces. Further, the system parameters used for the present study are described in detail below.

Let  $\omega_T$  is the average frequency of all SA-MTMFDs, given as

$$\omega_T = \sum_{j=1}^r \frac{\omega_j}{r} \quad (1)$$

where,  $r$  is the total number of SA-MTMFDs. The natural frequency  $\omega_j$  of the  $j^{th}$  SA-TMFD is expressed as

$$\omega_j = \omega_T \left[ 1 + \left( j - \frac{r+1}{2} \right) \right] \frac{\beta}{r-1} \quad (2)$$

where,  $\beta$  is the non-dimensional frequency spacing of the SA-MTMDs, given as

$$\beta = \frac{\omega_r - \omega_1}{\omega_T} \quad (3)$$

If  $K_{Td j}$  is the constant stiffness of each  $j^{th}$  SA-TMFD, then the mass of the  $j^{th}$  SA-TMFD is expressed as

$$m_{Td j} = \frac{K_{Td j}}{\omega_j^2} \quad (4)$$

The ratio of the total SA-MTMFDs mass to the total mass of the main system is defined as the mass ratio and is expressed as

$$\mu = \frac{\sum_{j=1}^r m_{Td j}}{m_s} \quad (5)$$

where,  $m_s$  denotes the total mass of the main system.

The ratio of average frequency of the SA-MTMFDs to the fundamental frequency of main system is defined as tuning ratio, expressed as

$$f = \frac{\omega_T}{\omega_s} \quad (6)$$

### III. EQUATIONS OF MOTION UNDER EARTHQUAKE EXCITATION

The governing equations of motion of multi-degree of freedom system (MDOF) with SA-MTMFDs when subjected to earthquake excitations are expressed as

$$M\ddot{X}_{(t)} + C\dot{X}_{(t)} + KX_{(t)} = E\ddot{x}_{g(t)} + BF_{d(t)} \quad (7)$$

where, the  $M$ ,  $C$  and  $K$  denotes the mass, damping and stiffness of the configured system, considered for the study.  $\ddot{X}_{(t)}$ ,  $\dot{X}_{(t)}$  and  $X_{(t)}$  are the relative acceleration, velocity and displacement vectors of the configured system relative to the ground.  $\ddot{x}_{g(t)}$  represents vector of the ground acceleration and  $F_{d(t)}$  represents the vector of the controllable friction forces provided by the SA-TMFDs. These matrices can be shown as:-

$$M = \begin{bmatrix} M_p & 0 \\ 0 & M_{Td} \end{bmatrix} \quad (8)$$

$$K = \begin{bmatrix} K_p + \sum_{j=1}^r K_{Td j} & -K_{Td1} & -K_{Td2} & -K_{Td3} & \dots & -K_{Td j} \\ -K_{Td1} & K_{Td1} & 0 & 0 & \dots & 0 \\ -K_{Td2} & 0 & K_{Td2} & 0 & \dots & 0 \\ -K_{Td3} & 0 & 0 & K_{Td3} & \dots & 0 \\ \vdots & \vdots & \vdots & \vdots & \ddots & \vdots \\ \vdots & \vdots & \vdots & \vdots & \vdots & 0 \\ -K_{Td j} & 0 & 0 & 0 & 0 & K_{Td j} \end{bmatrix} \quad (9)$$

$$C = \begin{bmatrix} C_p & 0 \\ 0 & 0 \end{bmatrix} \tag{10}$$

where,  $M_p$ ,  $K_p$  and  $C_p$  represents the square matrices of dimensions  $(n \times n)$ , denotes the mass, damping and stiffness of primary five storey structure and  $n$  denotes the degrees of freedom of the primary structure.  $M_{Td}$  denote the square matrix of dimension  $(r \times r)$ , where  $r$  is the number of SA-TMFD units.

It is also to be noted that as the damping matrix of the primary structure is not known explicitly, it can be constructed using the Rayleigh's damping considering it proportional to mass and stiffness of the primary structure as,

$$C_p = a_0 M_p + a_1 K_p \tag{11}$$

where  $a_0$  and  $a_1$  are the coefficients which depends on the damping ratio of two vibration mode. For the considered primary structure, damping ratio is taken as 2% for all the modes of vibration and,

$$F_d = \begin{bmatrix} \sum_{j=1}^r F_{dj} & -F_{d1} & -F_{d2} & \dots & -F_{dr} \end{bmatrix} \tag{12}$$

$$X_{(t)} = \begin{Bmatrix} x_{p(t)} \\ x_{td(t)} \end{Bmatrix} \quad \text{and} \quad Z_{(t)} = \begin{Bmatrix} X_{(t)} \\ \dot{X}_{(t)} \end{Bmatrix} \tag{13}$$

Here,  $x_{p(t)}$  represents the displacement of  $i^{th}$  floor of primary structure and  $x_{td(t)}$  represents the displacement of  $j^{th}$  SA-TMFD unit of SA-MTMFDs respectively, relative to the ground. Also, the matrix  $E$  and  $B$  are placement matrices for the excitation force and friction force, respectively.

**IV. SOLUTION OF EQUATIONS OF MOTION**

Equation (7) can be formulated in dynamic state space as

$$\dot{Z}_{(t+1)} = AZ_{(t+1)} + E\ddot{x}_{g(t+1)} + BF_{d(t+1)} \tag{14}$$

where, vector  $Z_{(t)}$  denotes the state of the system as shown in equation (13),  $F_{d(t)}$  denotes the vector of controllable friction forces provided by the SA-TMFDs,  $\ddot{x}_{g(t)}$  is the ground acceleration,  $A$  represents the system matrix that is composed of structural mass, stiffness and damping matrices. When the equation (15) is further discretized in the time domain assuming excitation force to be constant within any time interval, equation (15) can be converted into a discrete time form as mentioned by Meirovitch (1990).

$$Z_{(s+1)} = A_d Z_{(s)} + E_d \ddot{x}_{g(s)} + B_d F_{d(s)} \tag{15}$$

where, subscripts  $(s)$  and  $(s + 1)$  denotes that the variables are evaluated at the  $(s)^{th}$  and  $(s + 1)^{th}$  time step.

$$B_d = A^{-1}(A_d - I)B \tag{16a}$$

$$E_d = A^{-1}(A_d - I)E \tag{16b}$$

Also,  $A_d = e^{A\Delta t}$  denotes the discrete-time system matrix with  $\Delta t$  as the time interval.

Let  $y$  be a vector showing dampers displacements which are,  $y = x_{td(j)} - x_5$ , where  $x_{td(j)}$  denotes the displacement of  $j^{th}$  SA-TMFD of SA-MTMFDs and  $x_5$  denotes the displacement of the top i.e. fifth story. At any instant of time the relation between dampers displacements  $y$  and state of the structure  $Z$  may be written as

$$y_{(s)} = DZ_{(s)} \tag{17}$$

where,  $D$  is a constant matrix of dimension  $(r \times 2NR)$ ; where,  $NR = n + r$ , and  $n$  is the number of degrees of freedoms (DOFs) of the structure, and  $r$  is the total number of SA-TMFDs. Furthermore, each damper displacement consists of two components.

$$y_{(s)} = y_{r(s)} + y_{b(s)} \tag{18}$$

where,  $y_{r(s)}$  represents the slip displacement on the friction interfaces of the damper, while  $y_{b(s)}$  represents the elastic deformation of the damper, which are proportional to the axial force of the damper. The axial force of the FD are equivalent to the friction force, therefore, by the elastic constitutive law for axial member, we have

$$F_{d(s)} = K_{Td} \cdot y_{b(s)} \tag{19}$$

where,  $K_{Td}$  is a  $(r \times r)$  diagonal matrix consists of stiffness of the SA-TMFDs.

$$F_{d(s)} = K_{Td} [DZ_{(s)} - y_{r(s)}] \tag{20}$$

As it is clear from equation (20), the friction force vector  $F_{d(s)}$  is a function of the current structural state  $Z_{(s)}$  as well as the slip displacement on the friction interfaces of the two systems  $y_{r(s)}$ . At any given time instant each SA-TMFD unit of SA-MTMFDs can remain only in one state i.e. either in stick state or in slip state. During the time interval from  $(s - 1)^{th}$  to  $(s)^{th}$  time step, if each damper is in stick state then it should satisfy the following condition.

$$y_{r(s)} = y_{r(s-1)} \tag{21}$$

By applying the results of equations (20) and (21), the subtraction of  $F_{d(s-1)}$  and  $F_{d(s)}$  leads to

$$F_{d(s)} = K_{Td} D[Z_{(s)} - Z_{(s-1)}] + F_{d(s-1)} \tag{22}$$

Now, introducing equation (15) into equation (22) and replacing subscript  $(s)$  by  $(s - 1)$  leads to

$$\tilde{F}_{d(s)} = G_z Z_{(s-1)} + G_{xg} \ddot{x}_{g(s-1)} + G_{fd} F_{d(s-1)} \tag{23}$$

where,

$$\left. \begin{aligned} G_z &= K_{Td} D(A_d - I) \\ G_{xg} &= K_{Td} DE_d \\ G_{fd} &= K_{Td} DB_d + I \end{aligned} \right\} \tag{24}$$

Note that in equation (23),  $\tilde{F}_{d(s)}$  shows the damper forces computed by assuming that each damper is in stick state which may not be equal to actual friction force  $F_{d(s)}$ . As vector  $\tilde{F}_{d(s)}$  plays a very important role in deciding the state (either stick or slip) and actual friction force in the damper. It shows the minimum friction force required by the damper at the  $t^{th}$  time step to remain in stick state and thus it is referred as ‘critical friction force’. Equation (23) shows that vector  $\tilde{F}_{d(s)}$  can be computed easily, once  $Z_{(s-1)}$ ,  $F_{d(s-1)}$  and  $\ddot{x}_{g(s-1)}$  have been determined at the previous time step. Further, it is assumed that damper obeys Coulomb’s friction law. In this case the actual friction force vector  $F_{d(s)}$  and critical friction force vector  $\tilde{F}_{d(s)}$  shall be reduce to scalars  $F_{d(s)}$  and  $\tilde{F}_{d(s)}$ . The state of the damper can be decided to be

a) Stick state, if

$$|\tilde{F}_{d(s)}| < F_{d \max(s)} = F_c N_{(s)} \tag{25a}$$

b) Slip state, if

$$|\tilde{F}_{d(s)}| > F_{d \max(s)} = F_c N_{(s)} \tag{25b}$$

where,  $F_c$  is the friction coefficient and  $N_{(s)}$  is the time varying clamping force of the damper. Using these equations, once the state of the damper is determined, its frictional force can be calculated by

$$\left. \begin{aligned} F_{d(s)} &= \tilde{f}_{d(s)} \quad (\text{for stick state}) \\ F_{d(s)} &= \text{sgn}[\tilde{f}_{d(s)}] F_c N_{(s)} \quad (\text{for slip state}) \end{aligned} \right\} \quad (26)$$

where,  $\text{sgn}$  denotes the signum function which takes the sign of variable and is used to denote the direction of the resisting slip force. Once  $F_{d(s)}$  is obtained from equation (26) and substituted into equation (15), the structural response  $Z_{(s+1)}$  can be determined and then the response of the system in next time step can be simulated.

Equation (25b) shows that if the clamping force  $N_{(s)}$  is applied in such a way that resulting slip force is always slightly less than the value  $\tilde{F}_{d(s)}$  predicted by equation (23) then the damper will remain in the slip state for the complete duration of the harmonic or earthquake excitation. Based on this concept, the control rule for determining the clamping force of a semi-active friction damper is proposed by Lu (2004) as

$$N_{(s)} = \alpha \frac{|\tilde{F}_{d(s)}|}{F_c}, \quad 0 \leq \alpha \leq 1 \quad (27)$$

where,  $\alpha$  is a selectable constant parameter known as gain multiplier and  $\tilde{F}_{d(s)}$  is obtained from equation (23), substituting  $N_{(s)}$  from equation (27) into equation (25b), keeps the equation (25b) always true for each damper and keep each damper in its slip state. Therefore the damper friction forces can be computed by substituting equation (27) into equation (25) and re-writing it in a vector form as

$$F_{d(s)} = \alpha \tilde{F}_{d(s)} \quad (28)$$

Equation (28) shows that if the value of  $\alpha$  is such as  $0 \leq \alpha \leq 1$ , damper friction force vector  $F_{d(s)}$  will be always less than  $\tilde{F}_{d(s)}$ . By using equation (23) in equation (28), one can obtain an explicit formula to calculate the control forces vector as

$$F_{d(s)} = \alpha \left\{ G_z \cdot Z_{(s-1)} + G_{fd} \cdot F_{d(s-1)} + G_{xg} \cdot \ddot{x}_{g(s-1)} \right\} \quad (29)$$

From equation (29), it is noted that the parameter  $\alpha$  plays an important role in the proposed predictive control law.

## V. NUMERICAL STUDY

For the numerical study the five story shear type structure of fundamental time period of 0.5 sec is considered. The earthquake time histories along with their peak ground acceleration (PGA) and components which are used for this study are represented in Table 1. The displacement and acceleration response spectra of the above mentioned earthquakes are shown in Figure 2 for 2% critical damping. The maximum value of PGA are 1.225 g, 3.616 g, 3.296 g, 3.614 g, occurring at the period of 0.46 s, 0.64 s, 0.08 s and 0.36 s for Imperial Valley, Loma Prieta, Landers and Kobe earthquakes, respectively. The spectra of these ground motion indicate that these ground motions are recorded on a rocky site or on a firm soil. For the numerical study, the SA-MTMFDs are assumed to be attached to the top story of the structure as shown in Figure 1. The damping ratio of the primary system / structure is taken as 2%, constant for all modes of vibration. The weight of each floor is taken as 10000 kg. The natural frequencies of the structure are calculated as 2, 5.838, 9.203, 11.822, 13.484 Hz. The mass ratio,  $\mu$ , is taken as 5% of the total weight of the primary system. For the present study, the results are obtained with the interval,  $\Delta t = 0.02, 0.01$  and  $0.005$ , respectively. The number of iteration in each time step is taken as 50 to 200 to determine the incremental frictional force of the SA-TMFDs.

The controlling parameter  $\alpha$  on which the efficiency of SA-TMFDs depends and the controlling parameter  $R_f$  on which the efficiency of P-MTMFDs depends, are discussed here for a fair comparison between the two. For the study purpose all the considered system parameters of the configured system attached with P-MTMFDs and SA-MTMFDs are kept same. The response quantities of the interest considered for the study are peak values of displacement, acceleration of the top story of the structure and average damper displacement of all the SA-MTMFDs.

### 5.1 Effect of Controlling Parameters on the Performance of P-MTMFDs and SA-MTMFDs

To investigate the performance of P-TMFDs and SA-MTMFDs in response reduction of five story shear structure, the optimum number of P-TMFD units and SA-TMFD units in P-TMFDs and SA-TMFDs are found out respectively. For this purpose the number of P-TMFD unit and SA-TMFD unit is varied as 1, 5 and 11. Also, for a fair comparison of performance of P-TMFDs and SA-TMFDs, optimum values of their respective controlling parameters are found out.

To determine the optimum value of controlling parameter  $R_f$  and study its influence on the performance of P-MTMFDs, the value of  $R_f$  (i.e. maximum friction force of the damper normalized by the weight of the P-TMFD) is varied from 1 to 50%. The variation of peak displacement, peak acceleration of the top story and the average stroke of P-MTMFDs is plotted against  $R_f$  in Figures 3, 4 and 5, respectively. It is observed from Figure 3 and 4 that as the value of  $R_f$  increases the peak displacement and peak acceleration response of the top story decreases up to a certain point and further increases gradually with the increase in the value of  $R_f$ . It is also, observed from Figure 5 that as the value of  $R_f$  increases the average stroke of P-MTMFDs decreases. Further, the study of peak response reduction with respect to variation in average peak stroke with respect to same value of  $R_f$ , shows that the peak responses of structure decreases with the decrease in the value of average peak stroke up to a certain point and again gradually increases with further reduction in the average peak stroke. Thus, giving emphasis on the maximum reduction of peak responses of the structure and reasonable value of average stroke, the optimum value of  $R_f$  is chosen. The optimum value of  $R_f$  at which the response of the system attains its minimum value is taken as 2%, 4%, 0.1% and 7%, for Imperial Valley, Loma Prieta, Landers and Kobe earthquakes, respectively. The variation of the optimum value of  $R_f$  for different earthquake is due to their different dynamic characteristic. It is also, observed from the figures that there exist an optimum number of TMFD units in P-MTMFDs at which P-TMFDs perform effectively and reduces the responses of system. Further, it is to be noted that increasing the number of TMFD units is not desirable from the economical point of view, once the optimum number of TMFD units are obtained. The optimum number of P-TMFD unit in P-MTMFDs are taken as 5 TMFD units for Imperial valley, Landers, Kobe earthquakes and 11 TMFD units for Loma Prieta earthquake.

Similarly, to find out the optimum value of controlling parameter  $\alpha$  and study its influence on the performance of SA-MTMFDs, the value of  $\alpha$  is varied from 0.1 to 0.999. The peak displacement, peak acceleration of the top story and the average stroke and average friction force (i.e. average of maximum friction forces of the dampers normalized by the weight of the SA-TMFDs) developed in the SA-TMFDs are plotted against  $\alpha$  in Figure 6, 7, 8 and 9. It is observed from the Figures 6, 7, 8 and 9 that as the value of  $\alpha$  increases the top story displacement, top story acceleration and the average peak stroke decreases and average frictional force of the SA-MTMFDs increases. Also, at a value of  $\alpha$  which is extremely close to one, the peak displacement and peak acceleration of top story increases. Also, it is possible that at value of  $\alpha$  which is extremely close to one, the SA-MTMFDs may enter in stick state for certain time instants, which may affect the energy dissipation capacity of the SA-MTMFDs. Hence by selecting an appropriate value of  $\alpha$ , one can keep SA-TMFD continuously in slip mode and utilize its energy dissipation capacity effectively. Thus, for a given earthquake excitation an optimum value of  $\alpha$  exist at which the response of the system attains its minimum value. The optimum value of  $\alpha$  is chosen as 0.92, 0.9, 0.999 and 0.8, for Imperial Valley, Loma Prieta, Landers and Kobe earthquakes, respectively. It is also observed that an optimum value of number of SA-TMFD unit exists in SA-MTMFDs at which the SA-MTMFDs perform effectively. The optimum number of SA-TMFD unit in SA-MTMFDs is taken as 5 TMFD units for Imperial Valley, Landers, Kobe earthquakes and 11 TMFD units for Loma Prieta earthquake. Thus, from the above study, it is summarized as by selecting an appropriate value of  $\alpha$  one can keep SA-MTMFDs continuously in slip mode and utilize its energy dissipation capacity effectively. For a given earthquake excitation an optimum value of  $\alpha$  exists at which the response of the system attains its minimum value. The variation of the optimum value of  $\alpha$  for different earthquake is due to their different dynamic characteristic. Further, an optimum value of number of SA-TMFD unit exists in SA-MTMFDs at which the SA-MTMFDs perform effectively.

## 5.2 Effects of PGA

In order to study the effect of PGA on the responses of interest, the PGA of earthquake time histories are scaled from 0.05 g to 1g. The peak displacement and peak acceleration of the top story along with the average of peak damper displacement i.e. average peak stroke of a MDOF system with P-MTMFDs, SA-MTMFDs and uncontrolled system are plotted against the different PGA level for various earthquakes in Figures 10, 11 and 12. For a fair comparison, the responses of P-MTMFDs are plotted with the optimum number of P-TMFD units and optimum value of  $R_f$  for each earthquake as obtained in earlier section. Also, the responses of SA-MTMFDs are plotted with optimum number of SA-TMFD units and optimum values of  $\alpha$ . It is observed that both P-MTMFDs and SA-MTMFDs reduce the response of interest effectively. Even for some earthquakes optimally selected P-MTMFDs and SA-TMFDs performs at par. However for most of the earthquakes the response reduction ability of SA-TMFDs is higher than that of P-MTMFDs. It is also observed from the figure that sometimes at very low PGA levels like 0.05 g and 0.1 g the value of average peak stroke of P-MTMFDs is close to zero, which shows that at very low intensity earthquakes the P-MTMFDs hardly activates or underperforms. It is also observed that the SA-MTMFDs can be activated at all PGA levels and is also effective in reducing the response of the MDOF system at all PGA levels, due to this SA-MTMFDs overcomes all the limitations of P-MTMFDs.

In a similar manner, Figures 13, 14, 15 and 16 depict the displacement and acceleration time history of top story of the primary system attached with P-MTMFDs, SA-MTMFDs and uncontrolled system for optimum value of  $R_f$  and  $\alpha$  with optimum number of their respective TMFD units. For this purpose, the PGA of all the considered earthquakes is scaled to 0.4 g and 0.9 g, which shows the low and high intensity level earthquakes, respectively. The time history responses of the system confirms that the SA-MTMFDs are more effective than P-MTMFD in response reduction of the MDOF system as it is activated at such a lower and higher PGA levels.

## 5.3 Effect of Variation of Mass Ratio, Tuning Ratio and Frequency Spacing

Figures 17, 18 and 19 depict the effectiveness of control algorithm, when assuming the changes in the parameters or properties of the P-MTMFDs and SA-MTMFDs. For this purpose, the responses of P-MTMFDs and SA-MTMFDs is plotted against the varying mass ratio, tuning ratio and frequency spacing in Figures 17, 18 and 19, respectively. It is observed that the response of the system is relatively less sensitive to the change in mass ratio of the system. While, in case of change in the tuning property and frequency spacing of the system, it is more sensitive. It is also observed that the responses of interest are more sensitive for the SA-MTMFDs in compare to responses of P-MTMFDs having values of responses at lower side in compare to P-MTMFDs. So, even if the actual friction force applied at SA-MTMFDs is different (due to change in properties/ parameters like mass ratio, tuning ratio and frequency spacing of SA-MTMFDs) than that of the friction force calculated from Predictive control law, SA-MTMFDs slightly alters the responses of the system at lower side in compare to its passive counterpart, which ensures its better performance level in compare to P-MTMFDs.

## VI. CONCLUSIONS

The response of five story shear type structure attached with P-MTMFDs and SA-MTMFDs is investigated under four different seismic excitations. The predictive control law proposed by Lu (2004) is used for this study as it produces continuous and smooth slip force throughout the duration of an excitation. The governing differential equations of motion of the system are solved numerically, using state space method, to find out the response of the system. To investigate the effectiveness of SA-MTMFDs with predictive control, the responses of the system with P-MTMFDs are compared with the responses of the system with SA-MTMFDs. On the basis of trends of results obtained, the following conclusions are drawn:

1. By selecting an appropriate value of  $\alpha$  one can keep SA-MTMFDs continuously in slip mode and utilize its energy dissipation capacity effectively.
2. For a given earthquake excitation an optimum value of  $\alpha$  exists at which the response of the system attains minimum value. The variation of the optimum value of  $\alpha$  for different earthquake is due to their different dynamic characteristic.
3. An optimum value of number of SA-TMFD unit exists in SA-MTMFDs at which the SA-MTMFDs perform effectively.
4. SA-MTMFDs can be activated at all PGA levels and is also effective in reducing the response of the MDOF system at all PGA levels, due to this SA-MTMFDs overcomes all the limitations of P-MTMFDs.

- If the actual friction force applied at SA-MTMFDs is different (due to change in parameters like mass ratio, tuning ratio and frequency spacing of SA-MTMFDs) than that of the friction force calculated from predictive control law, SA-MTMFDs slightly alters the responses of the system at lower side in compare to its passive counterpart, which ensures its better performance level in compare to P-MTMFDs.

Earthquake	Recording Station	Component	Duration (Sec)	PGA (g)
Imperial Valley (19 <sup>th</sup> May 1940)	El Centro Array # 9	I – ELC 180	40	0.313
Loma Prieta (18 <sup>th</sup> October 1989)	UCSC 16 LOS Gatos Presentation Centre (LGPC)	LGP 000	25	0.96
Landers 28 <sup>th</sup> June 1992	Lucerene Valley	LCN 275	48.125	0.721
Kobe 16 <sup>th</sup> January 1995	Japan Meterological Agency (JMA) 99999 KJMA	KJM 000	48	0.82

Table 1: Details of Earthquakes considered for Numerical study.

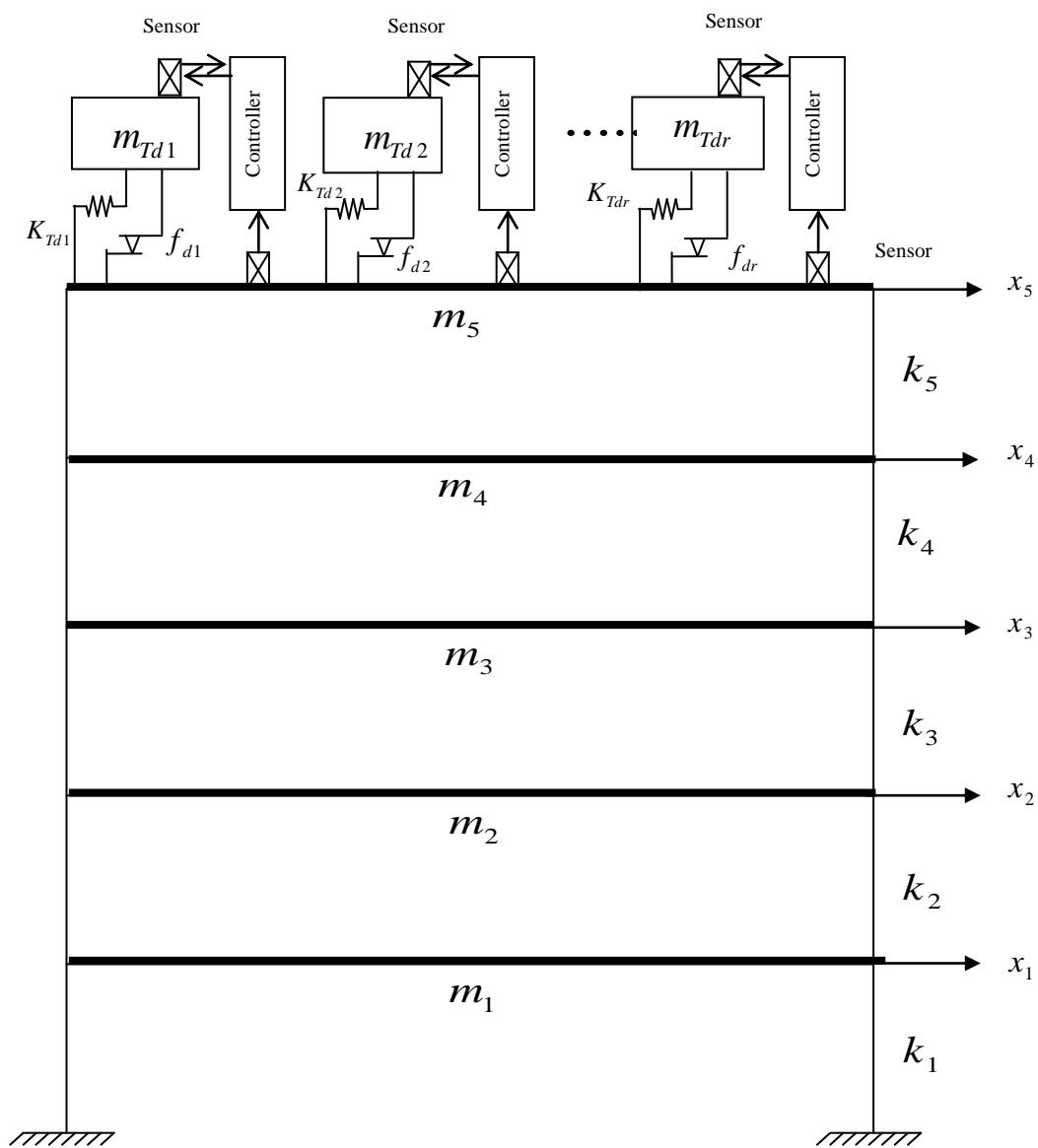


Figure 1: Schematic diagram of a multi-story structure with semi-active multiple tuned mass friction dampers.

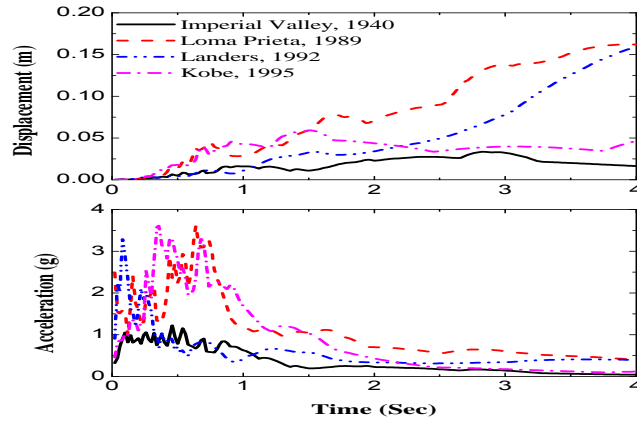


Figure 2: Displacement and acceleration spectra of the selected earthquakes.

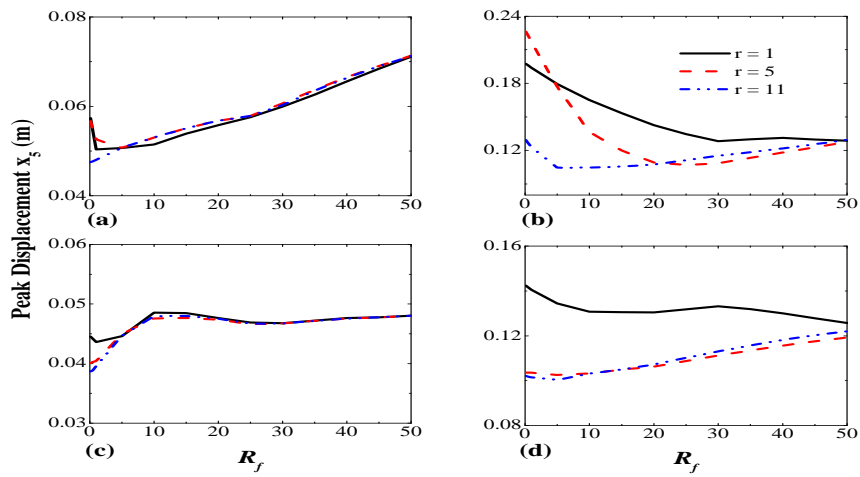


Figure 3: Influence of  $R_f$  on peak displacement on response of P-MTMFDs. (a) Imperial Valley, 1940; (b) Loma Prieta, 1989; (c) Landers, 1992; (d) Kobe, 1995.

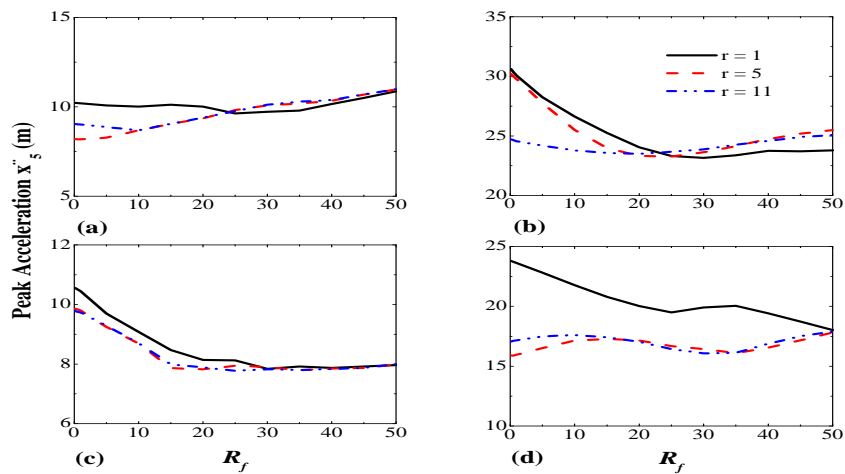


Figure 4: Influence of  $R_f$  on peak acceleration response of P-MTMFDs. (a) Imperial Valley, 1940; (b) Loma Prieta, 1989; (c) Landers, 1992; (d) Kobe, 1995.

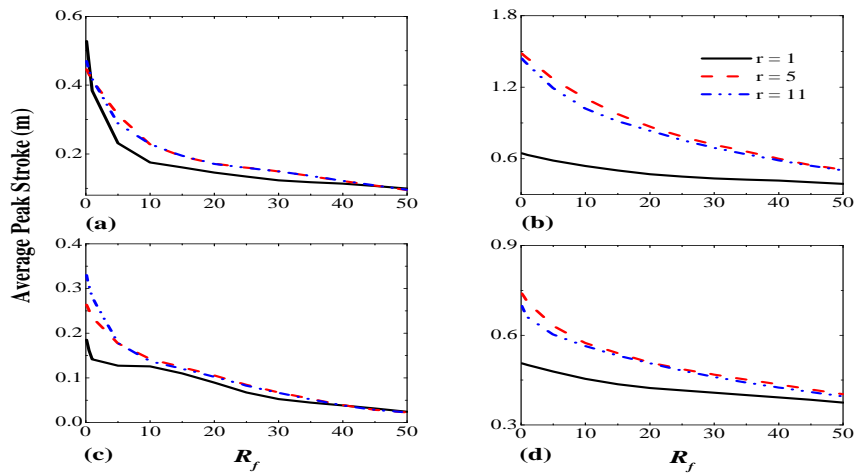


Figure 5: Influence of  $R_f$  on average peak stroke response of P-MTMFDs. (a) Imperial Valley, 1940; (b) Loma Prieta, 1989; (c) Landers, 1992; (d) Kobe, 1995.

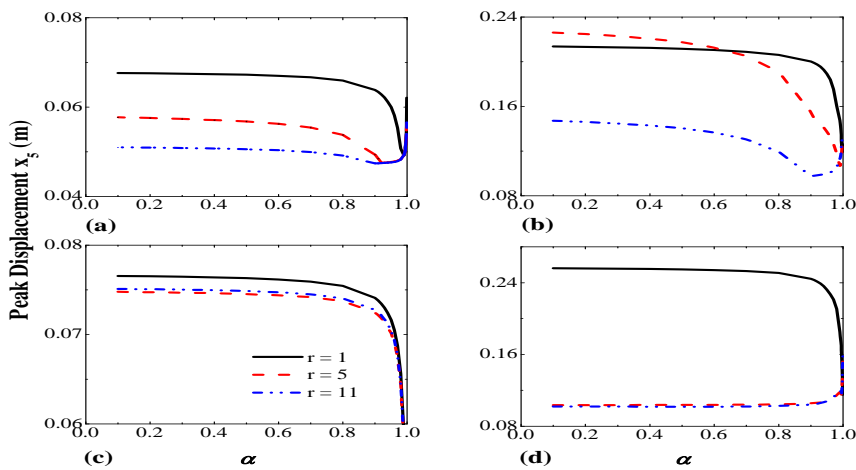


Figure 6: Influence of  $\alpha$  on peak displacement response of SA-MTMFDs. (a) Imperial Valley, 1940; (b) Loma Prieta, 1989; (c) Landers, 1992; (d) Kobe, 1995.

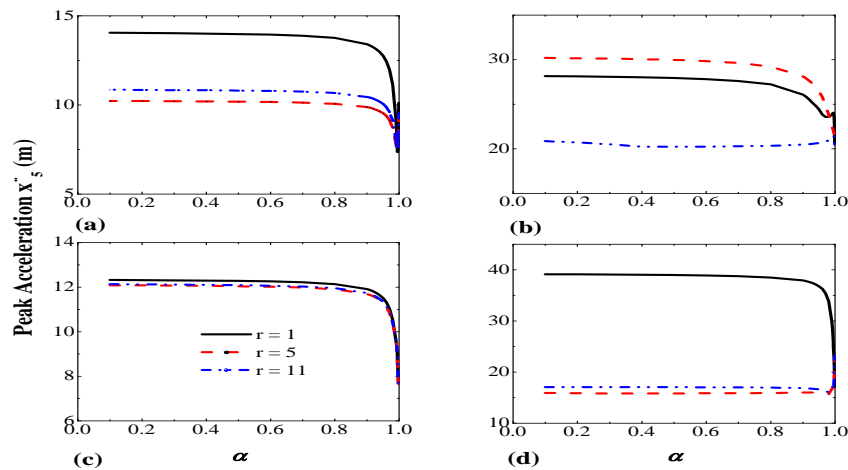


Figure 7: Influence of  $\alpha$  on peak acceleration response of SA-MTMFDs. (a) Imperial Valley, 1940; (b) Loma Prieta, 1989; (c) Landers, 1992; (d) Kobe, 1995.

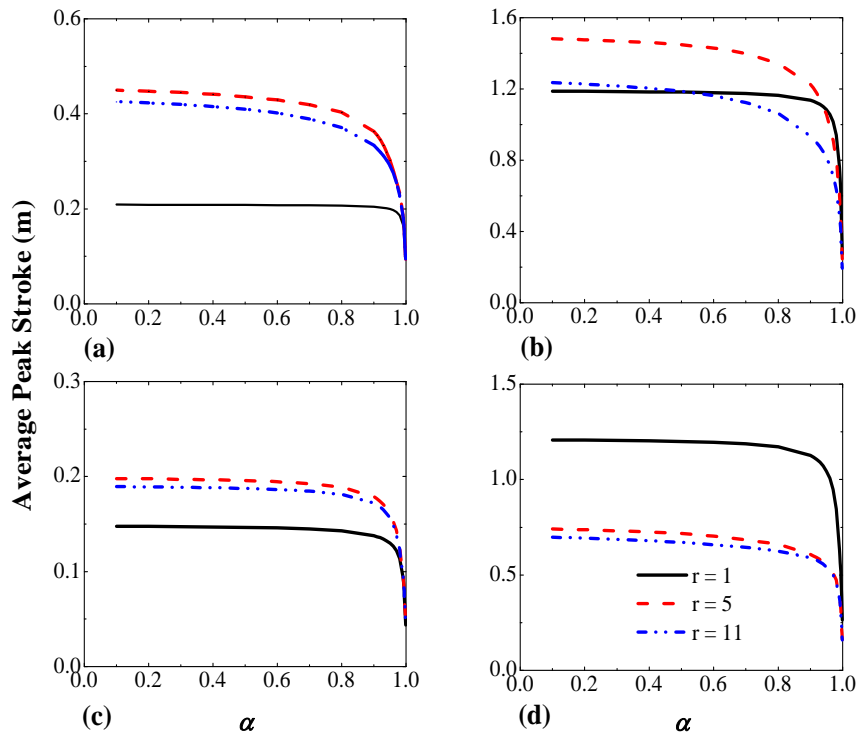


Figure 8: Influence of  $\alpha$  on average peak stroke response of SA-MTMFDs. (a) Imperial Valley, 1940; (b) Loma Prieta, 1989; (c) Landers, 1992; (d) Kobe, 1995.

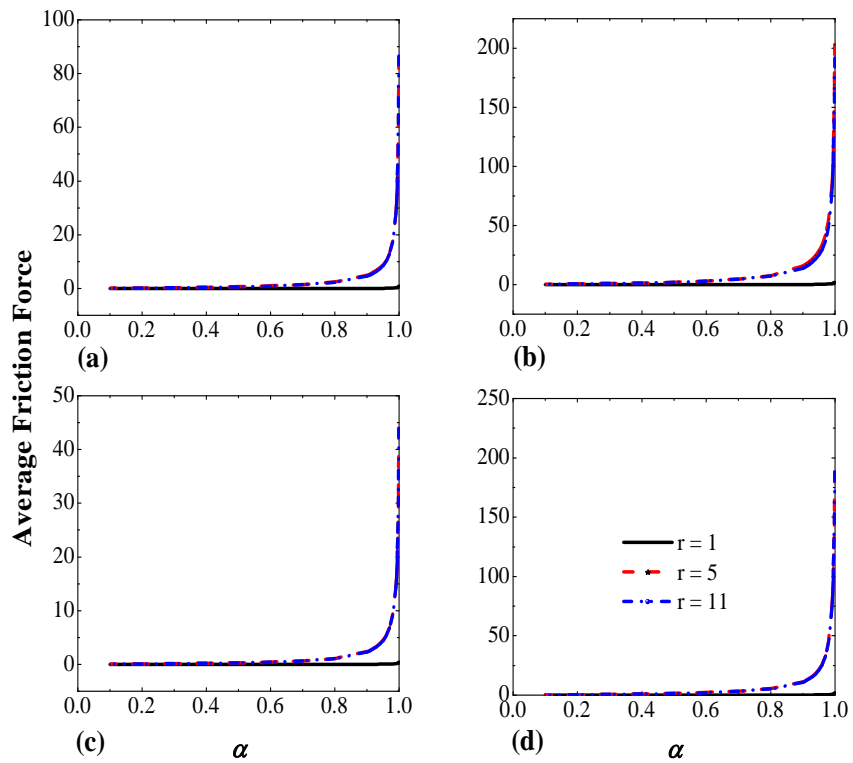


Figure 9: Influence of  $\alpha$  on average friction force of SA-MTMFDs. (a) Imperial Valley, 1940; (b) Loma Prieta, 1989; (c) Landers, 1992; (d) Kobe, 1995.

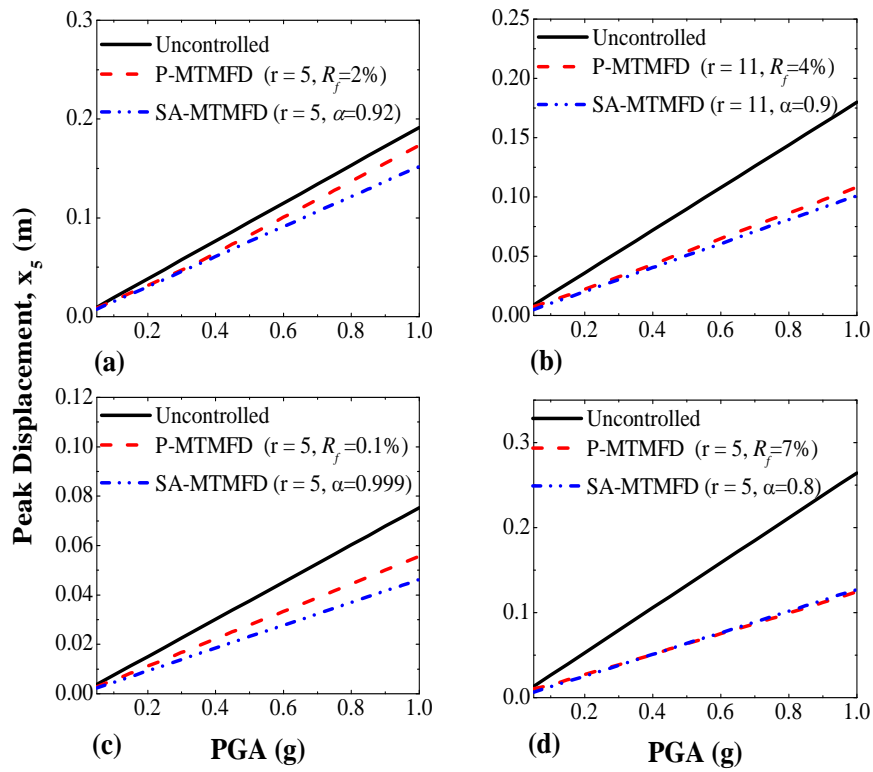


Figure 10: Peak displacement responses of P-MTMFDs and SA-MTMFDs under different Earthquakes. (a) Imperial Valley, 1940; (b) Loma Prieta, 1989; (c) Landers, 1992; (d) Kobe, 1995.

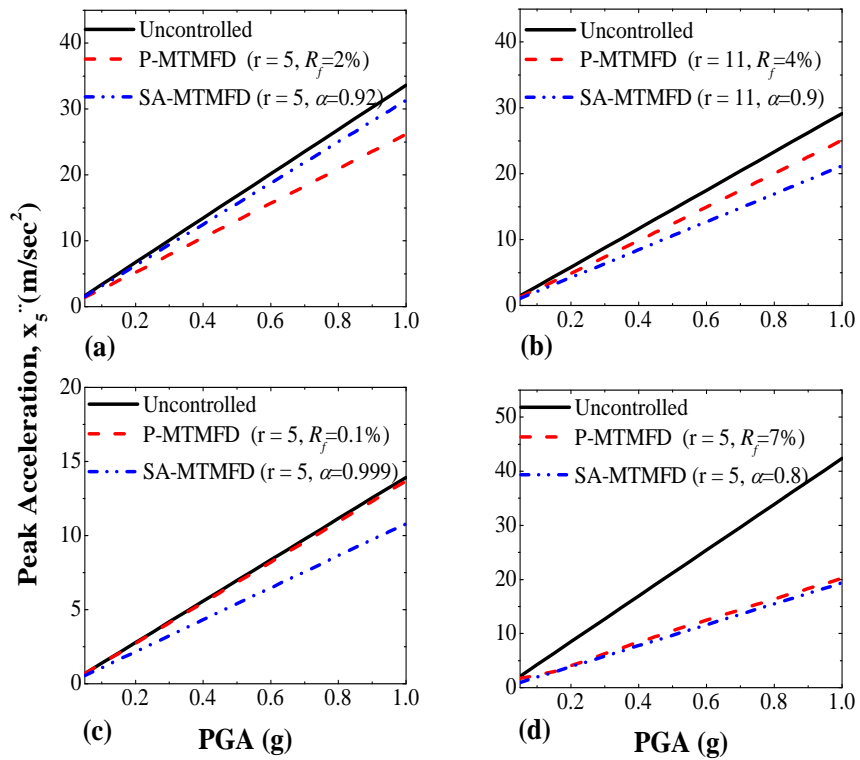


Figure 11: Peak acceleration responses of P-MTMFDs and SA-MTMFDs under different Earthquakes. (a) Imperial Valley, 1940; (b) Loma Prieta, 1989; (c) Landers, 1992; (d) Kobe, 1995.

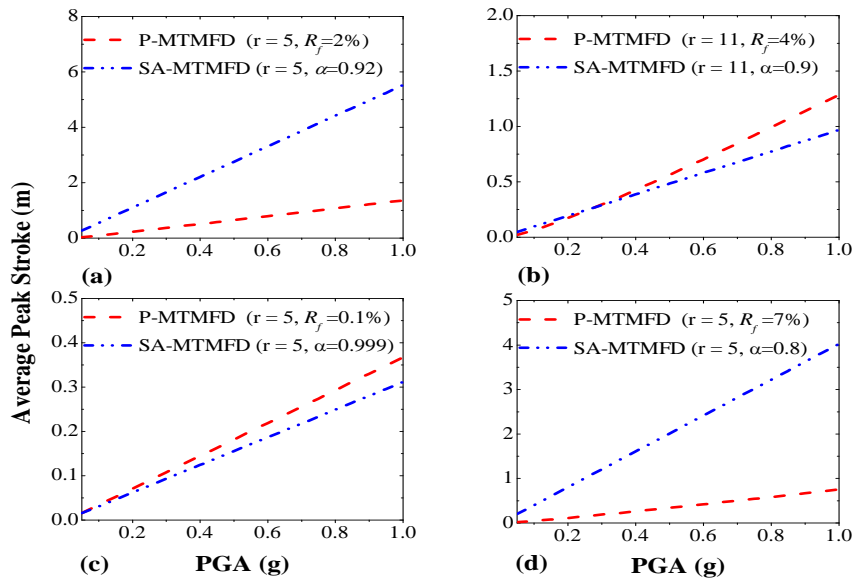


Figure 12: Peak average stroke responses of P-MTMFDs and SA-MTMFDs under different Earthquakes. (a) Imperial Valley, 1940; (b) Loma Prieta, 1989; (c) Landers, 1992; (d) Kobe, 1995.

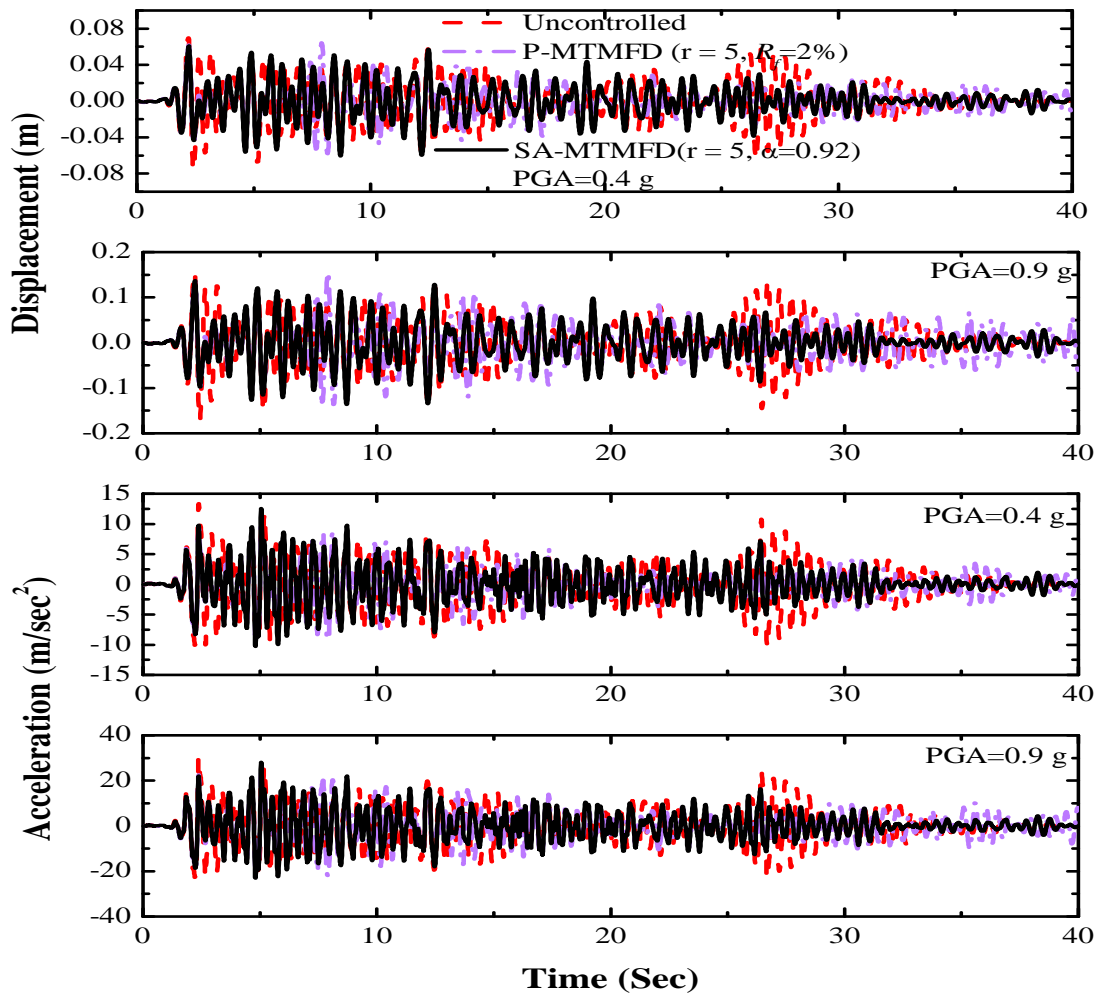


Figure 13: Comparison of Displacement & Acceleration responses of Uncontrolled, P-MTMFDs and SA-MTMFDs for Imperial Valley Earthquake (1940) for PGA as 0.4 g and 0.9 g.

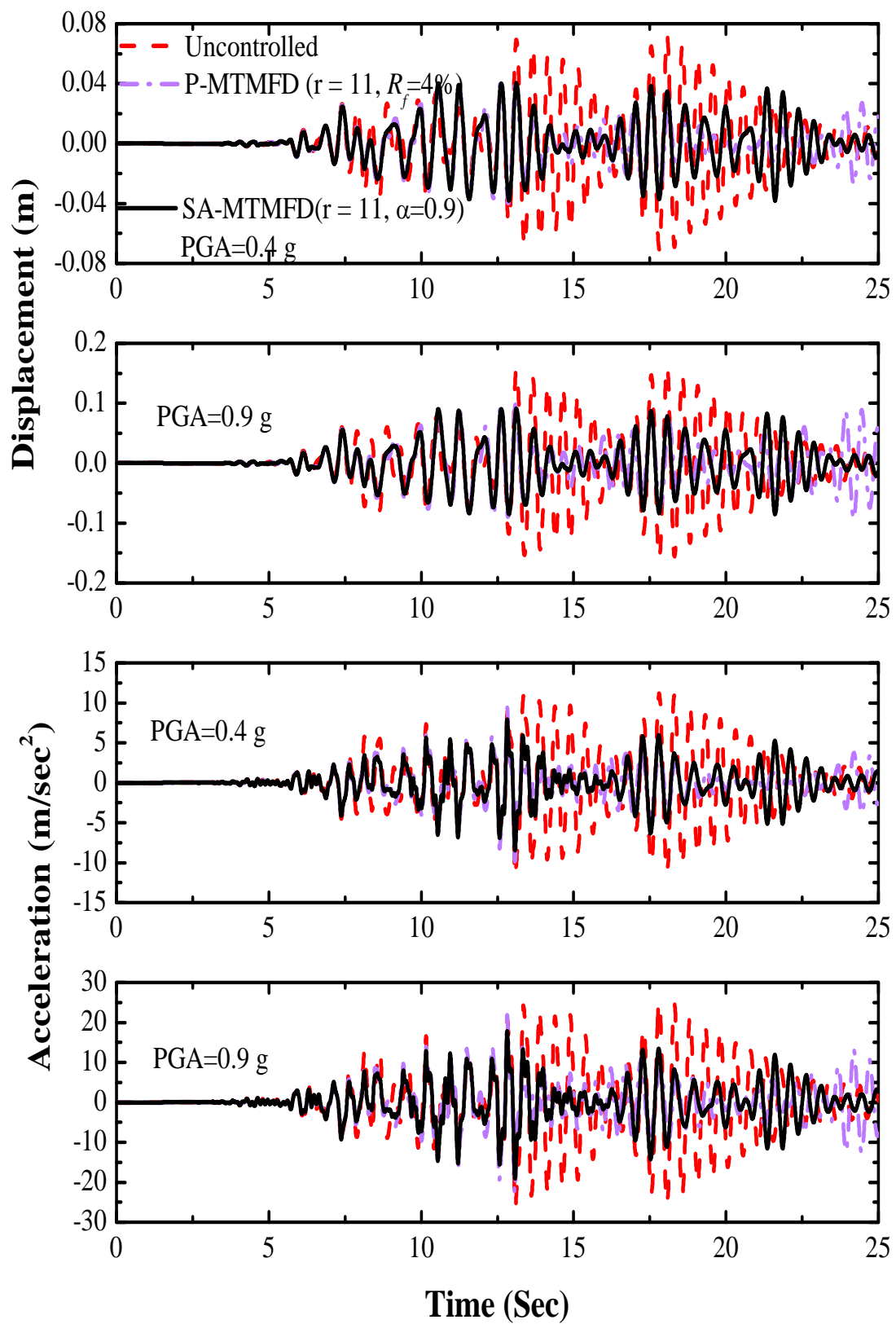


Figure 14: Comparison of Acceleration & Displacement responses of Uncontrolled, P-MTMFDs and SA-MTMFDs for Loma Prieta Earthquake (1989) for PGA as 0.4 g and 0.9 g.

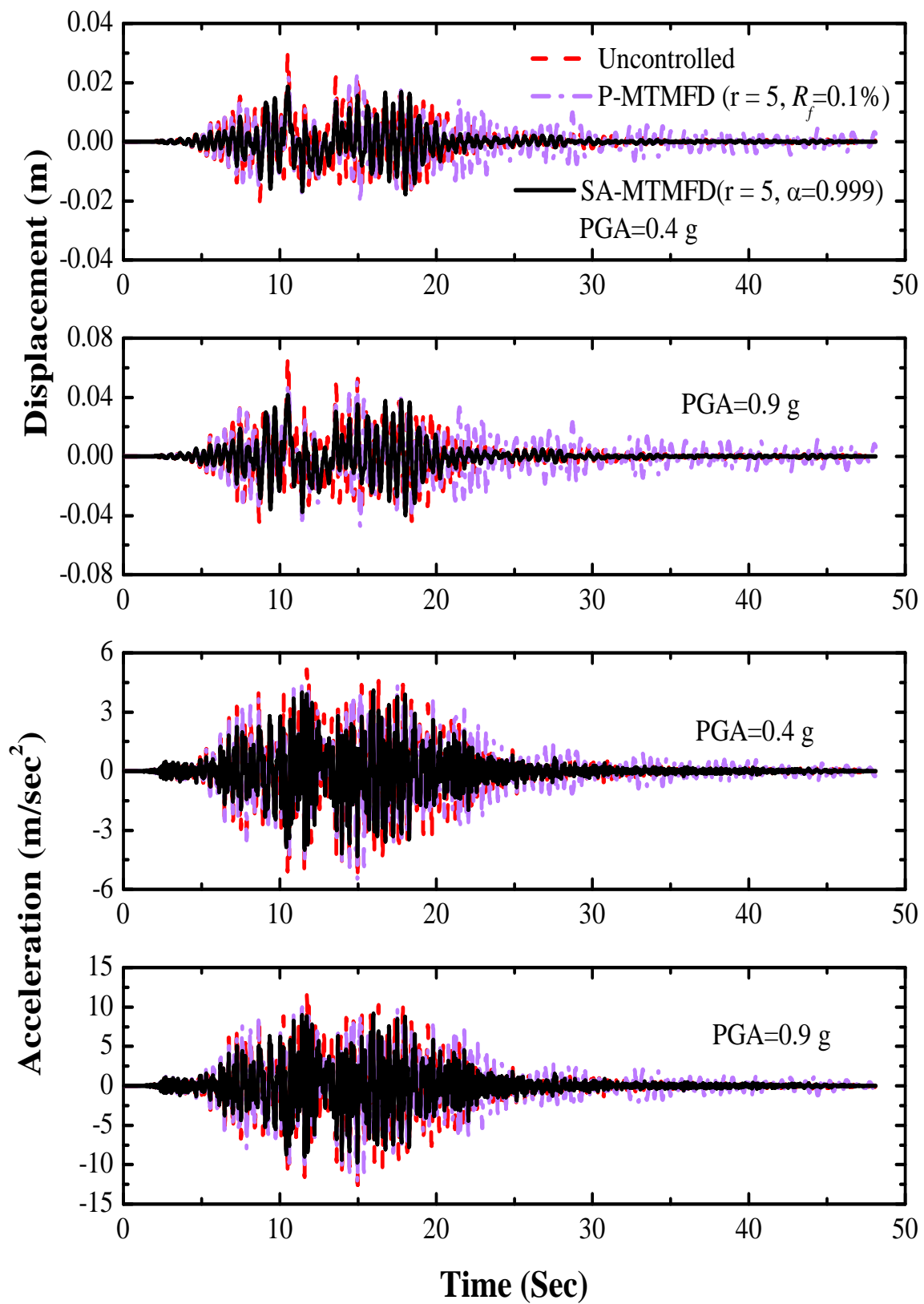


Figure 15: Comparison of Acceleration & Displacement responses of Uncontrolled, P-MTMFDs and SA-MTMFDs for Landers Earthquake (1992) for PGA as 0.4 g and 0.9 g.

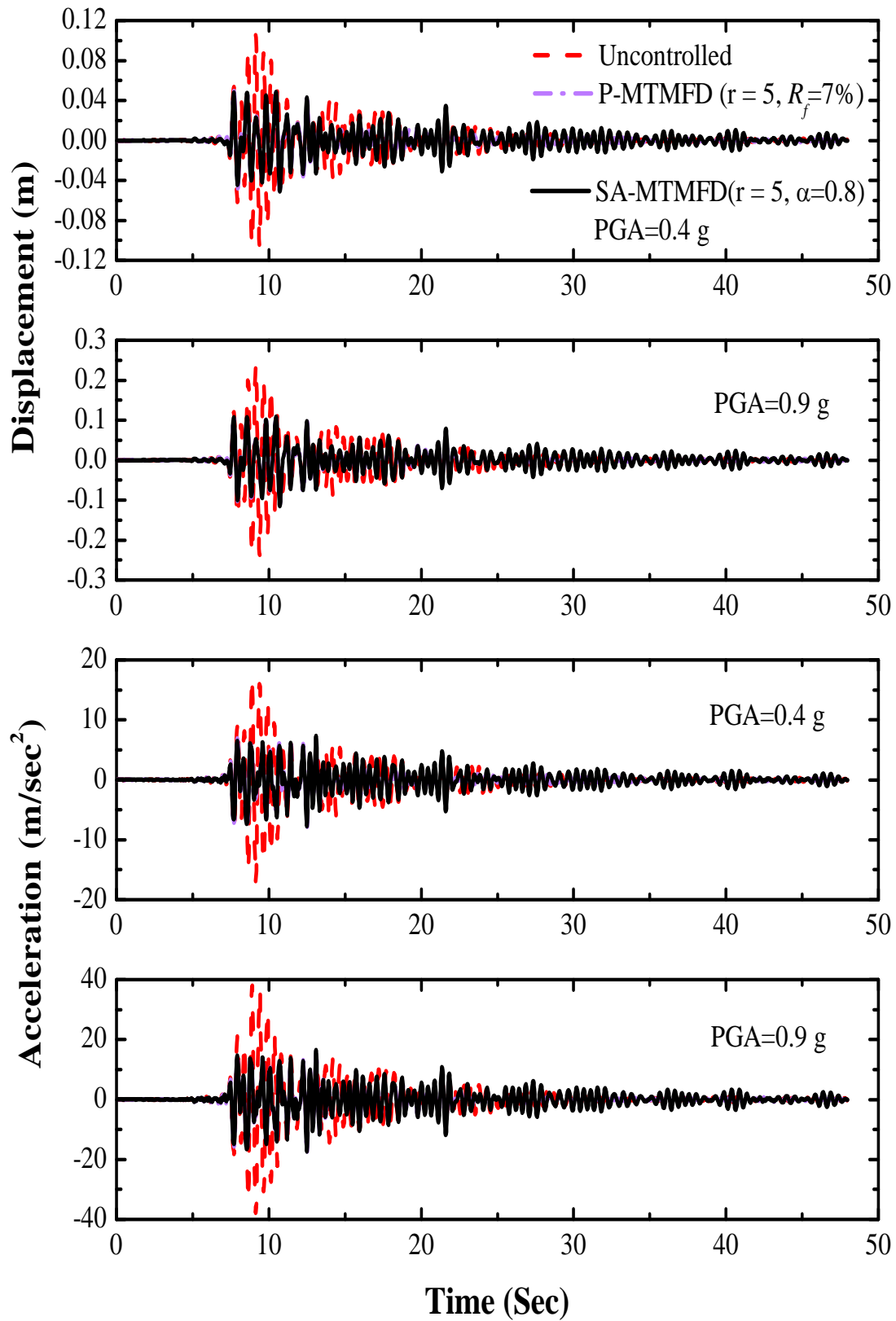


Figure 16: Comparison of Acceleration & Displacement responses of Uncontrolled, P-MTMFDs and SA-MTMFDs for Kobe Earthquake (1994) for PGA as 0.4 g and 0.9 g.

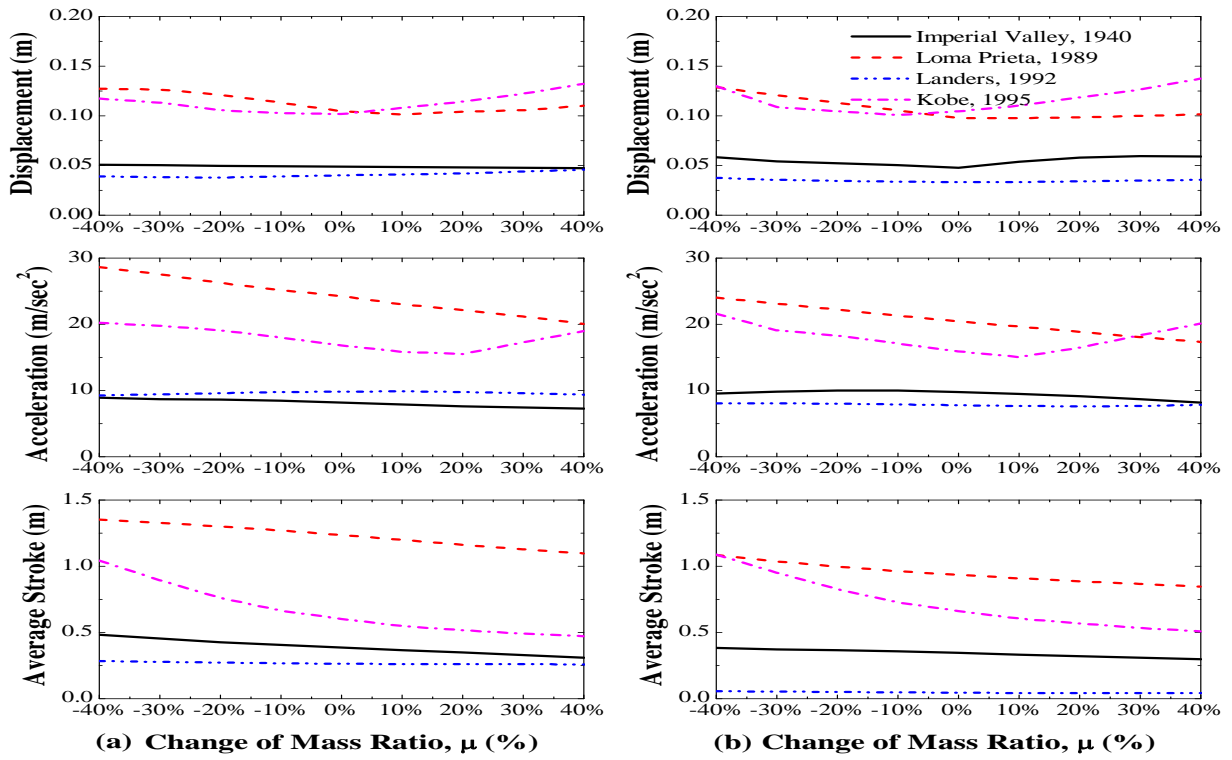


Figure 17: Effect of percentage variation in the mass ratio of P-MTMFDs and (b) SA-MTMFDs.

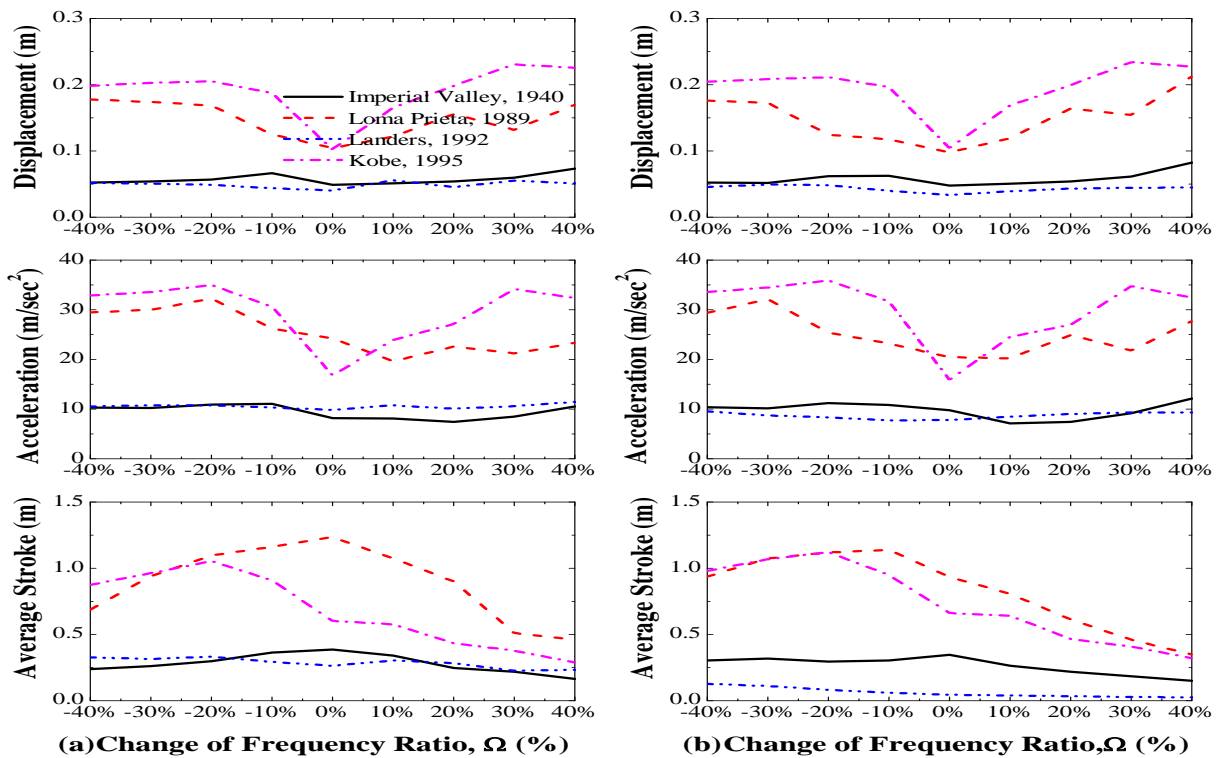


Figure 18: Effect of percentage variation in the frequency ratio of (a) P-MTMFDs and (b) SA-MTMFDs.

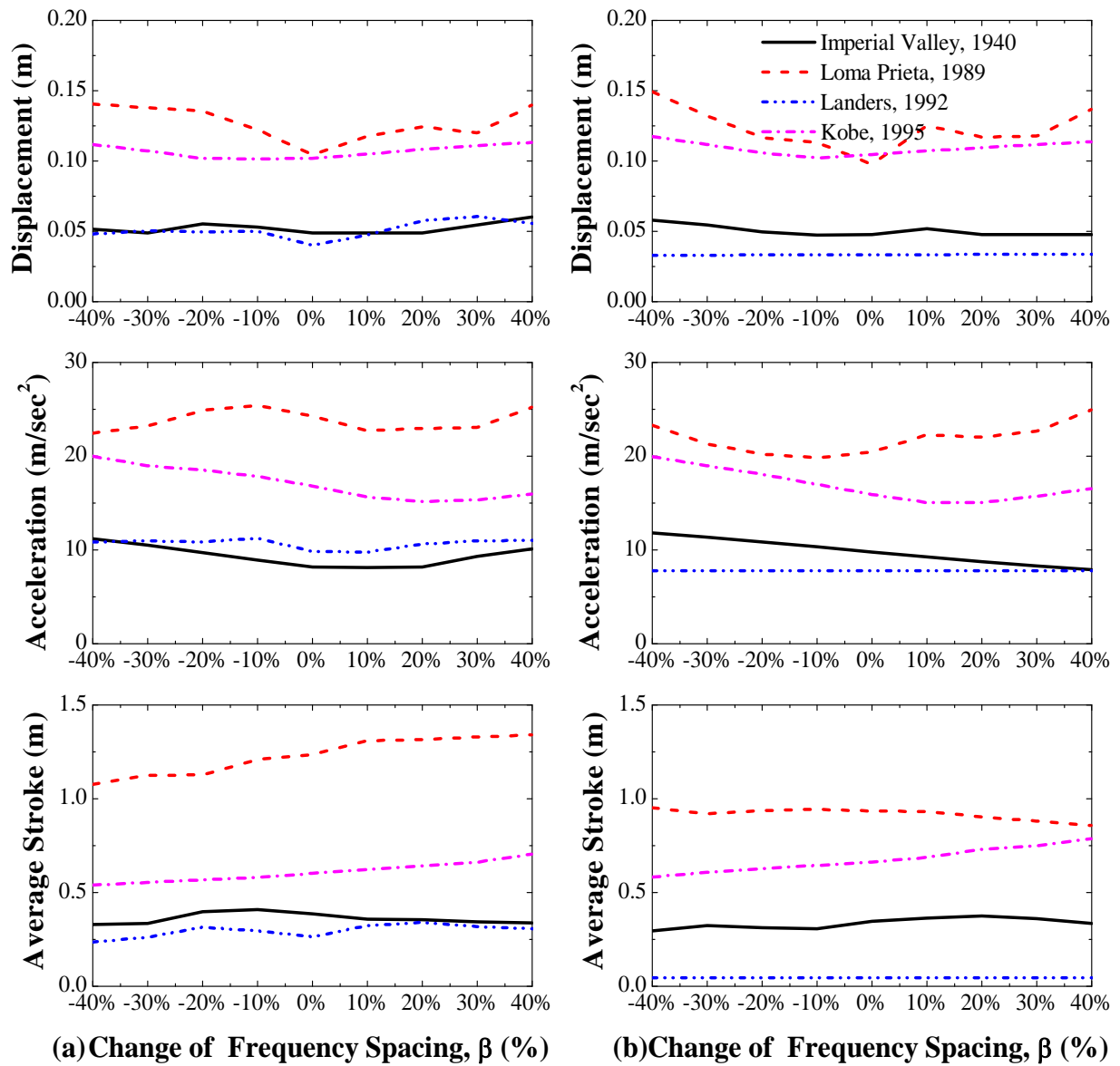


Figure 19: Effect of percentage variation in the frequency spacing of (a) P-MTMFDs and (b) SA-MTMFDs.

### REFERENCES

- [1] Z. Akbay and H.M. Aktan. Abating earthquake effects on buildings by active slip brace devices. *Shock and Vibration*, 2(2), 133-142, 1995.
- [2] P. Colajanni and M. Papia. Seismic response of braced frames with and without friction dampers. *Engineering Structures*, 17, 129-40, 1995.
- [3] D.J. Dowdell and S. Cherry. Structural control using semi-active friction dampers. *Proceedings of the First World Conference on Structural Control*, Los Angeles, Vol. 3; FAI-59-68, 1994.
- [4] Z. Gewei and B. Basu. A Study on friction-tuned mass damper: Harmonic solution and statistical linearization. *Journal of Vibration and Control*, 17, 721-731, 2010.
- [5] J.A. Inaudi. Modulated homogeneous friction: A semi-active damping strategy. *Earthquake Engineering and Structural Dynamics*, 26(3), 361-376, 1997.
- [6] A.S. Joshi and R.S. Jangid. Optimum parameters of multiple tuned mass dampers for base excited damped systems. *Journal of Sound and Vibration*, 202, 657-667, 1997.
- [7] S. Kannan, H.M. Uras and H.M. Aktan. Active control of building seismic response by energy dissipation. *Earthquake Engineering and Structural Dynamics*, 24(5), 747-759, 1995.
- [8] J.H. Lee, E. Berger and J.H. Kim. Feasibility study of a tunable friction damper *Journal of Sound and Vibration*, 283, 707-722, 2005.

- [9] C.C. Lin, G.L. Ling and J.F. Wang. Protection of seismic structures using semi-active friction TMD. *Earthquake Engineering and Structural Dynamics*, 39, 635-659, 2010.
- [10] L.Y. Lu. Predictive control of seismic structures with semi-active friction dampers. *Earthquake Engineering and Structural Dynamics*, 33(5), 647-668, 2004.
- [11] L. Meirovitch. *Dynamics and control of structures*, John Wiley & Sons, Inc., New York, 1990.
- [12] I.H. Mualla and B. Belev. Performance of steel frames with a new friction damper device under earthquake excitation. *Engineering Structures*, 24, 365-71, 2002.
- [13] C. Pasquin, N. Leboeuf, R.T. Pall and A.S. Pall. Friction dampers for seismic rehabilitation of Eaton's building. Montreal, 13<sup>th</sup> World Conference on Earthquake Engineering, Paper No. 1949, 2004.
- [14] W.L. Qu, Z.H. Chen and Y.L. Xu. Dynamic analysis of wind-excited truss tower with friction dampers. *Computers and Structures*, 79, 2817-31, 2001.
- [15] F. Ricciardelli and B.J. Vickery. Tuned vibration absorbers with dry friction damping. *Earthquake Engineering and Structural Dynamics*, 28, 707-723, 1999.
- [16] K. Xu and T. Igusa. Dynamic characteristics of multiple substructures with closely spaced frequencies. *Earthquake Engineering and Structural Dynamics*, 21(12), 1059-1070, 1992.